Polymer 49 (2008) 2077–2084

Contents lists available at ScienceDirect

Polymer

journal homepage: www.elsevier.com/locate/polymer

Theoretical studies of the electronic structures and optical properties of stable blue-emitting polymer based on 4*H*-cyclopenta-[*def*]-phenanthrene

Tao Liu [a], Hong-Xing Zhang [a,*], Bao-Hui Xia [a,b]

[a] State Key Laboratory of Theoretical and Computational Chemistry, Institute of Theoretical Chemistry, Jilin University, Changchun 130023, People's Republic of China
[b] College of Chemistry, Jilin University, Changchun 130023, People's Republic of China

ARTICLE INFO

Article history:
Received 6 January 2008
Received in revised form 24 February 2008
Accepted 26 February 2008
Available online 4 March 2008

Keywords:
Phenanthrene
DFT
Fluorescence

ABSTRACT

Geometries, ionization potentials (IPs), electron affinities (EAs) and optical properties of two series of π-conjugated oligomers (2,6-(4,4-bis(2-ethylthexyl)-4*H*-cyclopenta-[*def*]-phenanthrene))$_n$ **CPP***n* (2,6-(4,4-bis(2-ethylthexyl)-8,9-dihydro-4*H*-cyclopenta-[*def*]-phenanthrene))$_n$ **HCPP***n* ($n = 1$–4) were studied theoretically. The ground and the excited state geometries were optimized by B3LYP and CIS methods with 6-31G* basis sets, respectively. The absorption and the emission spectra were calculated by TD-B3LYP method. The lowest-lying absorption is assigned to $\pi \rightarrow \pi^*$ transition, and the fluorescence can be described as originating from the $^1[\pi\pi^*]$ excited state. IPs, EAs, H–L gaps, absorption and emission properties of **PCPP** ($n = \infty$) and **PHCPP** ($n = \infty$) were obtained by extrapolation method. The fact that the lowest-lying absorption and the emission of **PCPP** are blue-shifted compared with those of **PHCPP**, can be interpreted by the smaller effective repeating units of **PCPP**. The extra absorption band at 289 nm of **PCPP** is contributed by the $\pi \rightarrow \pi^*$ transition involving the extra π-conjugation C=C bond.

1. Introduction

In the past few decades, the optical properties of the π-conjugated organic polymer materials attracted considerably much attention because of the extensive applications such as semiconducting devices [1], photovoltaic components [2], organic light-emitting diodes (OLEDs) [3], thin film transistors [4], and chemical sensors [5]. Since the polymeric light-emitting diodes based on poly(*p*-phenylenevinylene) (PPV) were reported by Burroughes et al. [6], various kinds of conjugated polymers such as poly(*p*-phenylene) (PPP), poly(thiophene) (PT), Poly(thienylenevinylene)s (PTVs), poly(fluorene) (PF), poly(fluorenevinylene) (PFV), and PPV etc. and their derivatives have been developed for LEDs [7,8]. Conjugated polymers with large band gaps, especially PF and their derivatives have acquired much interest since they emit blue light and also enable full color via energy transfer to longer wavelength emitters [9]. However, one of the problems of using polyfluorenes (PFs) is their tendency to generate long wavelength emission around 550 nm because of the formation of the keto defect sites or aggregates/excimers, turning the desired blue emission color into the undesired blue-green emission and a drop of electroluminescence (EL) quantum efficiency [10].

Recently, two π-conjugated polymers poly(2,6-(4,4-bis(2-ethylthexyl)-4*H*-cyclopenta-[*def*]-phenanthrene)) **PCPP** and poly(2,6-(4,4-bis(2-ethylthexyl)-8,9-dihydro-4*H*-cyclopenta-[*def*]-phenanthrene)) **PHCPP** were synthesized by Suh et al. [11], and the UV–vis absorptions and fluorescence of **PCPP** and **PHCPP** were investigated. **PCPP** was applied in LEDs successfully because it can inhibit the oxidative degradation process of the 9-position in the PF materials by fixing the distance between the two benzene rings in the fluorine moiety and accordingly suppressing the development of green emission effectively, but **PHCPP** has similar optical properties just like PF because of the formation of keto defect. Interestingly, they found that the absorption and the fluorescence of **PCPP** are blue-shifted by fixing the distance with extra C=C double bond between the two benzene rings compared with the extra C–C single bond of **PCHPP**. They presumed that the extra π-conjugation between two benzene rings somehow alters the overall optical properties in a way different from simple effective conjugation length consideration. Furthermore, they estimated that the sharp absorption bands at 290 nm and 310 nm of **PCPP** are localized on extra π-conjugation C=C bond [11].

With the development of the quantum chemistry, the theoretical calculation can rationalize the properties of the materials and provide guidance to experimental works [12]. However, it is impossible to take the real polymer systems as the theoretical model object due to the limitation of the theory level and the vast size of the systems. This question was solved in 1987 by Lahti et al., who explored the extrapolation method [13] to investigate the excitation energy of several potentially conducting conjugated polymers, in

* Corresponding author. Tel.: +86 431 88498966; fax: +86 431 88945942.
E-mail address: zhanghx@mail.jlu.edu.cn (H.-X. Zhang).

0032-3861/$ – see front matter © 2008 Elsevier Ltd. All rights reserved.
doi:10.1016/j.polymer.2008.02.042

which a series of oligomers with different chain length were calculated, then the chain length were infinitely extrapolated to estimate the properties of the polymer. This approach is theoretically reliable since the conjugated oligomers have the characteristic to converge in geometries and electronic structures as well as the spectroscopic properties. Komatsu et al. [14], Ma et al. [15], Feng et al. [16], and Gierschner et al. [17] have successfully carried out the theoretical calculation to predict the various properties such as IPs, EAs, H–L gap, and the absorption and emission properties of polymer with the help of extrapolation method.

Herein, we selected the theoretical models with 1–4 repeating units which are marked as **CPP1** (monomer), **CPP2** (dimer), **CPP3** (trimer) and **CPP4** (tetramer), and corresponding **HCPP1**, **HCPP2**, **HCPP3** and **HCPP4**. To save the computation resources, we used the hydrogen atoms to replace the alkyl groups on 9-position appearing in the real molecules [11] since the alkyl substituents hardly influence the spectral properties. Indeed, it is a general technique to employ the hydrogen atom to replace the methyl, phenyl, butyl, etc. in the calculation [18–20] for the simplification. A sketch of the chemical structures of **PCPP** and **PHCPP** models is depicted in Fig. 1. The ground and the excited state geometries, electronic structures, IPs, EAs, H–L gap, absorption and the fluorescence properties of **CPP***n* and **HCPP***n* ($n = 1$–4) were explored theoretically, aiming at obtaining the properties of **PCPP** and **PHCPP** by extrapolation method. Through the comparison between **PCPP** and **PHCPP**, the origin of the unusual blue-shift and the properties of the sharp absorption band around 300 nm of **PCPP** were revealed.

2. Computational details and theory

Previously, the properties of π-conjugated polymer were always studied by semi-empirical methods such as AM1 and ZINDO approaches due to that. these methods are not expensive and can be performed on the large molecular systems, but the exact quantitative estimation of the electronic properties can hardly be obtained because of the insufficient description of the electron correlation effects and the use of empirical parameters [16,21]. In recent years, density functional theory (DFT) [22] method has attracted considerable much attention because this method can consider the electronic correlation very well and can be applied to the large systems. Recent studies by Orti et al. [23] showed that B3LYP [24] (Becke's three parameter functional and the Lee–Yang–Parr functional) scheme is remarkably successful in resolving a wide variety of polymer systems, and it can yield the similar and reliable geometries for medium sized molecules as MP2 calculations done [15,16,25,26].

Configuration interaction singles (CIS) [27,28] method, presenting a general zeroth-order treatment to excited state just as HF for the ground state of molecular systems, was successful in the structure optimization of the excited state proved by many researchers [16,29]. The wave function, energy, and analytic gradient of a molecule in an electronic excited state are available for the CIS method [28,30,31]. However, the transition energies obtained by the CIS calculations are usually overestimated since the CIS method uses the orbitals of a HF state in an ordinary CI procedure to solve for the higher roots and only considered parts of the electronic correlation effects via the mixing of excited determinants [30,31]. In our work, we rectified the excited state properties by time-dependent DFT (TD-DFT) method [31,32] to compensate the flaw of the CIS method.

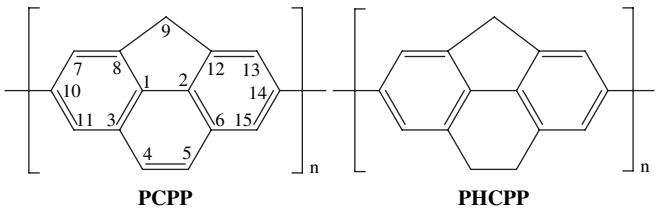

Fig. 1. Sketch structures of **PCPP** and **PHCPP**.

In our calculations, the ground and excited state geometries of **CPP***n* and **HCPP***n* ($n = 1$–4) were fully optimized by B3LYP and CIS methods, respectively, with the 6-31G* basis set. C_2 symmetry was adopted to settle the conformations of these models both in the ground and excited states. IPs, EAs, and H–L gap of them were also calculated by DFT method. The vertical absorptions and fluorescence were calculated by TD-DFT approach based on the ground and excited state optimized geometries, respectively. All of the calculations were carried out with Gaussian 03 software package [33] on an IBM server.

In our calculation, IPs and EAs are the differences of the energies between the ionic and the neutral molecules. The vertical IPs and EAs (labeled as v) were calculated based on the optimized geometry of the neutral molecule while the corresponding adiabatic data (labeled as a) were obtained based on the optimized geometry of the neutral and ionic molecules. We employed the extrapolation approach to acquire the certain properties of the polymer. We found that the present systems are more suitable adopting the binomial mode defined as $Y = a + bX + cX^2$, where X is equal to the reciprocal value of the repeating unit numbers, Y is the value of certain property [29a]. As shown in infra parts, the binomial mode can offer more precise extrapolation value in contrast to that of the monomial mode. All parameters correlative to the electronic structures such as IPs (a, v), EAs (a, v), HOMO–LUMO (H–L) gap, and the optical properties of the polymers were obtained through the binomial mode extrapolation method.

3. Results and discussion

3.1. The ground state geometries

The main optimized geometry parameters of **CPP***n* and **HCPP***n* ($n = 1$–4) are listed in Table 1. As examples, the optimized geometries of **CPP4** and **HCPP4** are shown in Fig. 2. Vibrational frequencies were also calculated based on the optimized geometries of **CPP***n* and **HCPP***n* ($n = 1$–4) to verify that each of the geometries is a minimum (no minus frequency) on the potential energy surface. Table 1 shows that the calculated dihedral angles C(3)–C(1)–C(2)–C(6)/C(1)–C(3)–C(4)–C(5)/C(3)–C(4)–C(5)–C(6) of **CPP***n* and **HCPP***n* are almost 0.0°, indicating that the geometry keeps planar within repeating unit, but the calculated dihedral angles C(7)–C(10)–C(14)–C(13) are about 140°, which indicates that the whole molecules are not planar (except **CPP1** and **HCPP1**) but of a screw type structure, due to that, this kind of arrangement can minimize the steric effect and stabilize the molecules at the largest extent. Thus, we can propose that **PCPP** and **PHCPP** should be of screw structures. With respect to **CPP1**–**CPP4**, Table 1 shows that the bond lengths C(1)–C(2), C(4)–C(5), C(9)–C(8)/C(9)–C(12), and C(3)–C(4)/C(5)–C(6) are 1.41 Å, 1.38 Å, 1.54 Å, 1.45 Å, respectively, within normal range of C–C and C=C [16]. These bond lengths are sorted in the order of **CPP1** > **CPP2** > **CPP3** > **CPP4** with the increase of the repeating units, and **HCPP***n* have the similar variation trends. For **HCPP***n*, the bond lengths C(1)–C(2), C(4)–C(5), and C(3)–C(4)/C(5)–C(6) are relaxed by about 0.02 Å, 0.20 Å, and 0.08 Å compared with the corresponding bond length of **CPP***n*, but C(9)–C(8)/C(9)–C(12) is hardly changed in relative to that of **CPP***n*. These variations of the bond lengths are the result of the changing of C(4)–C(5) bond type from C=C to C–C, thus C(4)–C(5) has the most obvious change about 0.20 Å. But the bond length of C(10)–C(14) is hardly changed with the variation of C(4)–C(5) bond type. Compared with **CPP***n*, the bond angles C(1)–C(3)–C(4) of **HCPP***n* are increased by about 3° and the C(3)–C(4)–C(5) are

Table 1
The optimized geometry structural parameters of **CPP1–CPP4** and **HCPP2–HCPP4** in the ground state (X^1A) under the B3LYP and the excited state (A^1B) under CIS level

	X^1A/A^1B							
	PCPP1	**PCPP2**	**PCPP3**	**PCPP4**	**PHCPP1**	**PHCPP2**	**PHCPP3**	**PHCPP4**
Bond lengths (Å)								
C(1)–C(2)	1.410/1.406	1.408/1.382	1.407/1.366	1.407/1.378	1.437/1.368	1.435/1.403	1.434/1.422	1.433/1.399
C(4)–C(5)	1.382/1.434	1.382/1.360	1.382/1.358	1.382/1.359	1.588/1.574	1.588/1.562	1.588/1.562	1.589/1.563
C(9)–C(8)/C(9)–C(12)	1.542/1.535	1.543/1.538	1.544/1.539	1.544/1.539	1.537/1.536	1.538/1.535	1.538/1.535	1.539/1.536
C(3)–C(4)/C(5)–C(6)	1.449/1.405	1.450/1.452	1.450/1.459	1.450/1.455	1.529/1.511	1.529/1.521	1.529/1.524	1.529/1.522
C(10)–C(14)		1.491/1.427	1.491/1.456	1.491/1.434		1.489/1.426	1.489/1.454	1.489/1.437
Bond angles (°)								
C(1)–C(3)–C(4)	115.3/115.4	115.2/114.9	115.1/114.3	115.1/114.7	118.2/114.8	118.1/115.7	118.1/115.9	118.0/115.4
C(3)–C(4)–C(5)	122.1/122.1	122.1/122.2	122.1/122.2	122.1/122.3	117.5/113.7	117.6/114.4	117.6/114.7	117.5/114.3
C(8)–C(9)–C(12)	102.9/102.5	102.9/102.6	102.9/102.6	102.9/102.6	102.9/102.3	102.9/102.6	102.9/102.6	102.9/102.5
C(7)–C(10)–C(14)		119.2/120.5	119.0/120.0	119.1/120.4		119.9/121.0	119.9/120.5	119.9/120.8
Dihedral angles (°)								
C(3)–C(1)–C(2)–C(6)	0.0/0.0	0.3/0.3	0.7/0.9	0.7/0.8	0.0/4.0	0.3/6.1	0.3/6.3	0.7/5.5
C(1)–C(3)–C(4)–C(5)	0.0/0.0	0.1/0.2	0.2/0.4	0.3/0.2	0.0/32.3	0.3/28.6	0.3/27.4	0.1/29.0
C(3)–C(4)–C(5)–C(6)	0.0/0.0	0.1/0.1	0.1/0.3	0.1/0.2	0.1/44.6	0.1/40.8	0.1/38.9	0.1/40.7
C(7)–C(10)–C(14)–C(13)		139.41/165.5	139.3/154.3	140.2/162.4		140.4/166.6	141.3/155.7	141.2/162.5

Fig. 2. The ground (a, c) and the excited (b, d) state geometries of **CPP4** (a, b) and **HCPP4** (c, d).

decreased by 3°, which is also the result of the variation of the bond C(4)–C(5), but the bond angles of C(8)–C(9)–C(12) and C(7)–C(10)–C(14) are hardly changed.

3.2. The frontier molecular orbitals

The energies of the frontier molecular orbitals of **CPP*n*** and **HCPP*n*** are given in Table 2. We plotted the contour plots of the HOMO and LUMO orbitals of **CPP2**, **CPP4**, and **HCPP4** in Fig. 3 as examples. Fig. 3 shows that the HOMO and LUMO of **CPP4** and **HCPP4** spread over the whole π-conjugated backbones with similar character, the HOMO displays *anti*-bonding character between two adjacent fragments and bonding character within repeating units. But the LUMO exhibits the bonding character between the two adjacent fragments and *anti*-bonding within the benzene rings. There is a tendency for HOMO and LUMO to populate the electrons in the middle repeating units, and the populations on the end units are deceased with the increasing unit number. Taking **CPP4** for example, with respect to HOMO, two terminal **CPP** fragments take only 27.0% compositions (population analysis using the SCF density), and the terminal **CPP** parts of LUMO have 28.0% compositions, while the middle **CPP** parts occupy more than 70.0% compositions. Fig. 3 shows that the composition of end repeating unit of **HCPP4** (30.0%) is bigger than that of **CPP4**, which indicates that the π conjugate effect of **HCPP*n*** is better than **CPP*n***. Fig. 3 also shows that the C(4)–C(5) single or double bond have little contribution to the HOMO and LUMO densities, which is consistent with the calculation results obtained by Ratner and co-workers on Phenanthrene dithiol (BP1) [34].

Table 2 shows that the HOMO and LUMO energies have a trend to converge namely, the HOMO energies increases and the LUMO energies decrease to an extremum with the repeating unit numbers increase to infinitude. Take **CPP*n*** for example, we found that the shift of HOMO energy ($\Delta\varepsilon_{HOMO}$) drops from an initial step of 0.22 eV (between **CPP1** and **CPP2**) to 0.13 eV (between **CPP2** and **CPP3**) and to 0.07 eV (between **CPP3** and **CPP4**) (see Table 2).

Table 2
The ionization potentials (eV), electron affinities (eV), H–L gap (eV), HOMO, LUMO, the lowest-lying absorptions and emissions (eV) of **PCPP** and **PHCPP** under the B3LYP calculations

	CPP*n*					**HCPP***n*				
	$n=1$	$n=2$	$n=3$	$n=4$	$n=\infty$	$n=1$	$n=2$	$n=3$	$n=4$	$n=\infty$
IP(v)	7.38	6.71	6.36	6.15	5.46	7.20	6.34	5.96	5.78	5.12
IP(a)	7.28	6.59	6.26	6.08	5.45	7.07	6.07	5.65	5.38	4.58
EA(v)	−0.67	−0.11	0.22	0.36	0.98	−1.17	−0.37	0.01	0.35	1.24
EA(a)	−0.51	0.01	0.34	0.53	1.22	−0.86	0.11	0.52	0.78	1.56
H–L	4.72	4.41	4.16	4.03	3.48	5.04	4.20	3.88	3.75	3.28
HOMO	−5.71	−5.49	−5.36	−5.29	−5.03	−5.52	−5.11	−4.96	−4.89	−4.66
LUMO	−0.99	−1.08	−1.19	−1.26	−1.53	−0.47	−0.91	−1.07	−1.14	−1.38
Absorption	4.32	3.81	3.67	3.60	3.42	4.71	3.83	3.48	3.34	2.82
Emission	4.02	3.46	3.26	3.16	2.87	4.11	3.21	2.97	2.87	2.60

The values of $\Delta\varepsilon_{HOMO}$ become smaller with the increasing chain length and the same variation trend is observed for the LUMO. **HCPP***n* has the similar variation trend to **CPP***n*. Table 2 also shows that whether in **CPP***n* or in the corresponding **HCPP***n*, the HOMO–LUMO gaps are narrowed gradually, which implies that it is easier to promote an electron from the HOMO to the LUMO with the increasing chain length. Interestingly, the HOMO–LUMO gaps of **CPP***n* are bigger than those of the corresponding **HCPP***n* except for **CPP1** despite the extra π-conjugated C═C bond in **CPP***n*, which is consistent with the composition of the frontier molecular orbitals, but it is contrast to the normal conclusion that the H–L gap can be decreased by increasing π-conjugated chain length [14–16,35].

Fig. 4 shows that there is a good binomial relationship between the H–L gaps and the inverse repeating unit numbers $1/n$ for **CPP***n* and **HCPP***n*. Through the extrapolation method, we obtained the H–L gap of **PCPP** (3.48 eV) and **PHCPP** (3.28 eV). The H–L gap of

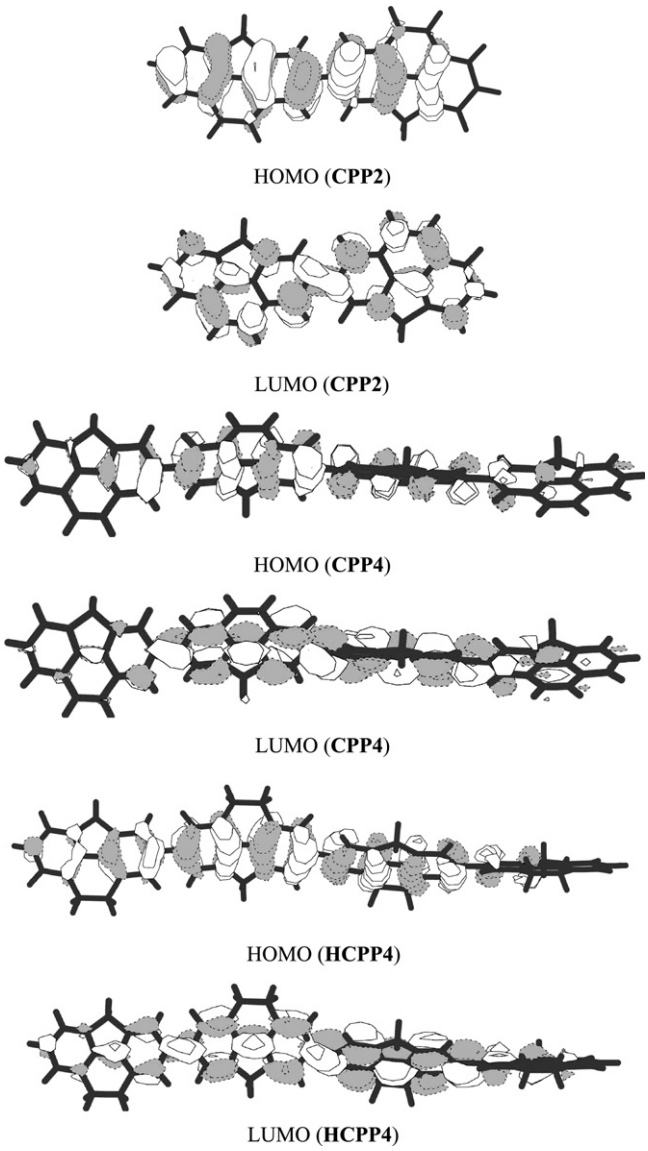

Fig. 3. Electron density diagrams of the HOMO and LUMO of **CPP2**, **CPP4** and **HCPP4**.

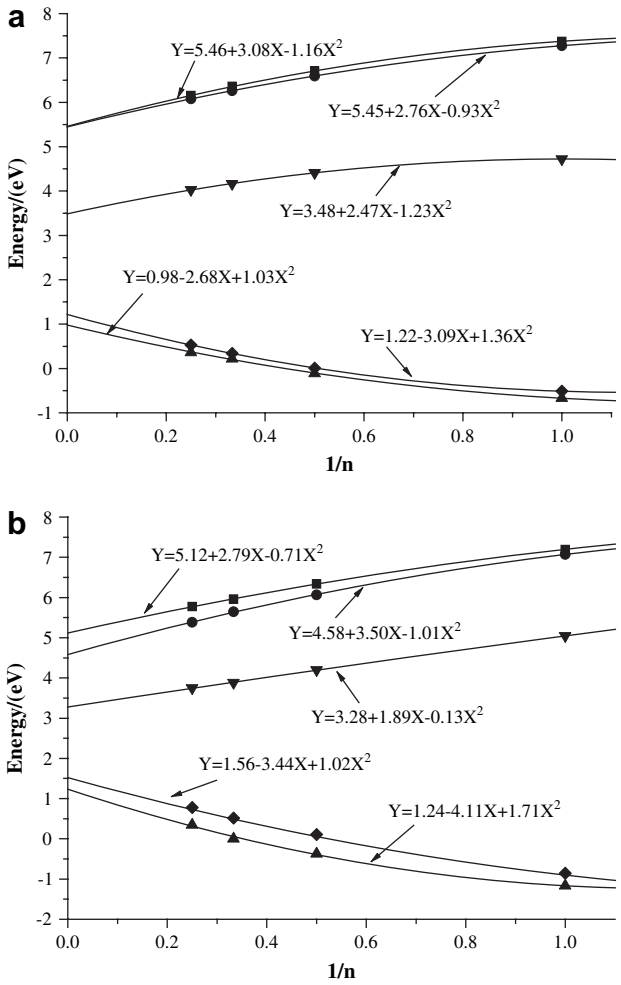

Fig. 4. Δ_{H-L}▼, IP(v)■, IP(a)●, EA(v)▲, and EA(a)◆ as a function (Y) of reciprocal chain length $1/n$ (X) for **CPP1**–**CPP4** (a) and **HCPP1**–**HCPP4** (b) under the B3LYP calculations.

polyfluorene calculated at B3LYP/6-31G level by Wang et al. [16a] is 2.91 eV, about 0.4 eV lower than our systems. The HOMO of **PCPP** (−5.03 eV) is lower than that of **PHCPP** (−4.66 eV), which indicated that the hole-accepting properties of **PCPP** is lower than that of **PHCPP**. The LUMO of **PCPP** and **PHCPP** are −1.53 eV and −1.38 eV, respectively, indicating that the electron-accepting abilities of **PCPP** is improved compared with **PHCPP**.

3.3. Ionization potentials and electron affinities

The calculated IPs(v, a) and EAs(v, a) are listed in Table 2. The values of the IPs(v, a) progressively decrease while the EAs(v, a) turn high gradually from $n = 1$ to $n = 4$. The values of IPs and EAs show good binomial relationship with $1/n$. Fig. 4 and Table 2 show that when the chain length is infinitely elongated to $n = \infty$, the vertical and adiabatic energies of **PCPP** required to extract an electron from the neutral molecule are 5.46 and 5.45, and those of **PHCPP** are 5.12 and 4.58 eV, which indicates that **PHCPP** is easier to lose an electron to create a hole than **PCPP**. The EA(v/a) energies needed to accept an electron are nearly 0.98/1.22 and 1.24/1.56 eV for **PCPP** and **PHCPP**, respectively, which means that **PHCPP** is apt to accept electrons compared with **PCPP**. Thus, **PHCPP** is more suitable for hole-creating and electron-accepting than **PCPP**.

3.4. Absorption spectra

The calculated dipole-allowed absorptions associated with the excitation energies, oscillator strength, and relative weight are listed in Table 3, the simulated Gaussian type absorption spectra of **CPP***n* and **HCPP***n* are shown in Fig. 5, and the simulated Gaussian type absorption spectra of **CPP4** and **HCPP4** are shown in Fig. 6. The simulated spectra appear to be similar in shape with the measured ones [11] except some red-shifts. The lowest-lying absorption excitation energy of **PCPP** and **PHCPP** obtained by extrapolation method are shown in Fig. 7. The density diagram plots of the

Table 3
The calculated dipole-allowed absorptions for **PCPP1**–**PCPP4** and **PHCPP2**–**PHCPP4** obtained by TD-B3LYP calculations

	Transition	λ, nm (eV)	Oscillator	Relative weight (%)
CPP1	H → L (0.60)	287 (4.32)	0.1003	73.5
	H-1 → L + 1 (0.51)	245 (5.06)	0.2784	53.1
CPP2	H → L (0.48)	325 (3.81)	0.0540	47.0
	H-1 → L + 1 (0.50)	282 (4.40)	0.7651	51.0
	H-4 → L + 1 (0.41)	225 (5.52)	0.2903	34.3
CPP3	H → L (0.63)	333 (3.72)	1.0620	81.0
	H-3 → L + 1 (0.47)	286 (4.33)	1.5685	45.1
	H-4 → L + 4 (0.54)	254 (4.89)	0.5765	59.5
CPP4	H → L (0.66)	344 (3.60)	2.0968	88.9
	H-4 → L + 1 (0.49)	289 (4.29)	1.8463	49.0
	H-5 → L + 2 (0.33)			22.2
	H-1 → L + 5 (0.44)	277 (4.48)	0.4527	39.5
	H → L + 6 (0.39)			31.0
	H → L + 8 (0.56)	258 (4.81)	0.2005	64.0
HCPP1	H → L (0.64)	263 (4.71)	0.3286	83.6
	H → L + 2 (0.59)	189 (6.57)	0.6657	71.0
HCPP2	H → L (0.67)	324 (3.83)	1.2106	91.6
	H-3 → L + 5 (0.40)	192 (6.44)	1.2984	32.7
	H-2 → L + 4 (0.32)			20.9
	H-4 → L + 5 (0.32)			20.9
HCPP3	H → L (0.67)	356 (3.48)	1.9893	91.6
	H-1 → L + 1 (0.67)	272 (4.56)	0.4257	91.6
	H-4 → L + 1 (0.41)	218 (5.68)	0.0774	34.3
	H-1 → L + 7 (0.40)			32.7
	H-1 → L + 6 (0.23)			10.8
HCPP4	H → L (0.67)	371 (3.34)	2.7064	91.6
	H-1 → L + 1 (0.66)	300 (4.14)	0.6387	88.9
	H-2 → L + 2 (0.53)	249 (4.97)	0.1373	57.3

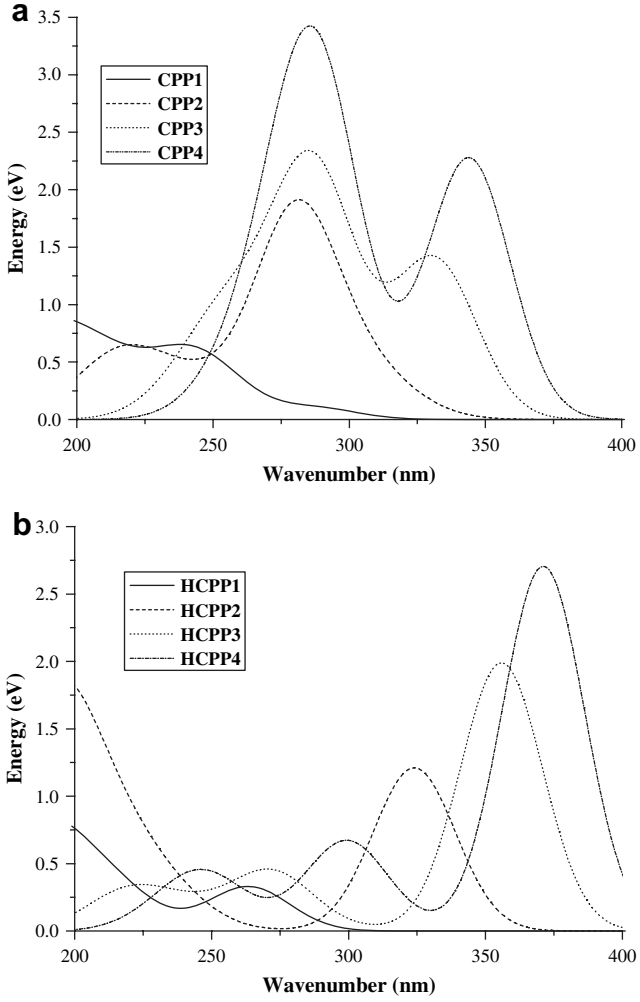

Fig. 5. (a) The Gaussian type absorption spectra for **CPP1**–**CPP4**; (b) the Gaussian type absorption spectra for **HCPP1**–**HCPP4**.

absorption transitions for **CPP4** and **HCPP4** are shown in Figs. 8 and 9 to help understanding the excitation processes.

Table 3 shows that the lowest-lying absorption bands at 287, 325, 333, 344 nm of **CPP1**–**CPP4** and 263, 324, 356, 371 nm of **HCPP1**–**HCPP4**, are all from the electron excitation from HOMO to LUMO. Take **CPP4** as example, Table 3 and Fig. 3 show that HOMO is a π type orbital which is dominantly localized on the middle two repeating units, with the composition of 70.0%, and the LUMO also distributes on the middle of the molecule with π^* character. The frontier orbitals of other **CPP***n* and **HCPP***n* have the similar character with **CPP4**. Therefore, the lowest-lying absorption transitions of **CPP***n* and **HCPP***n* are all assigned to $\pi \rightarrow \pi^*$ type transitions (see Figs. 8a and 9a). Furthermore, the lowest-lying absorptions are progressively red-shifted and the oscillator strength increased from **CPP1** to **CPP4** and from **HCPP1** to **HCPP4**, because of the increasing π-conjugation chain length which is consistent with our previous paper [29a]. Moreover, the excitation energy drops ($\Delta n = 1$) of **CPP***n* and **HCPP***n* become small like the Δ_{H-L} gaps. The extrapolation results showed that the excitation energy of the lowest-lying absorption at 363 nm (3.42 eV) of **PCPP** is higher than that at 439 nm (2.82 eV) of **PHCPP**, which is consistent with the H–L gap results. On experiment, the absorption at 350 nm of **PCPP** and 380 nm of **PHCPP** are both assigned to $\pi \rightarrow \pi^*$ type transitions, which is consistent with our calculated results [11]. Compared within **CPP***n* or **HCPP***n*, the lowest-lying absorptions are red-shifted with the increase of the repeating unit numbers.

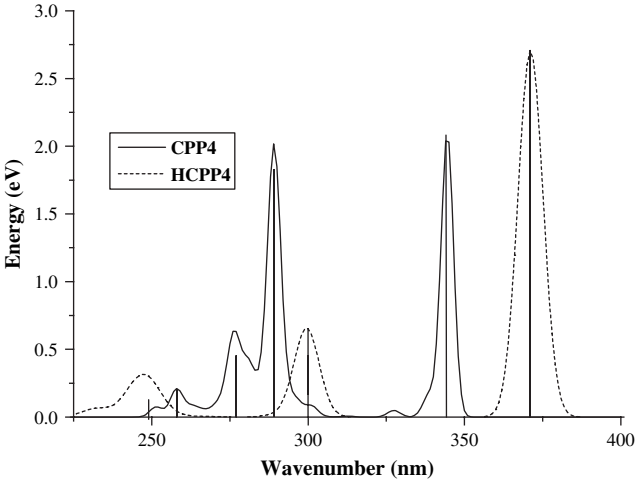

Fig. 6. The Gaussian type absorption spectra for **CPP4** and **HCPP4**.

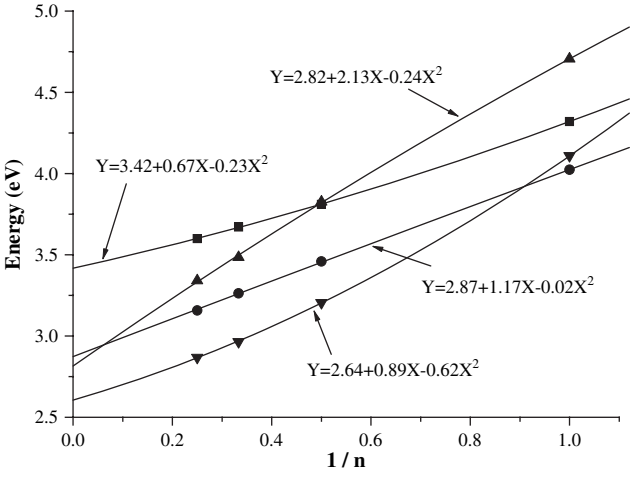

Fig. 7. The lowest-lying absorption energy of **CPP***n* ■ and **HCPP***n* ▲, the lowest-energy emission energy of **CPP***n* ● and **HCPP***n* ▼ as a function (*Y*) of reciprocal chain length 1/*n* (*X*) under the B3LYP calculations.

But the lowest-lying absorption of **PCPP** (363 nm) has an abnormal blue-shift compared with that of **PHCPP** (439 nm), which is contrast to the well-known conclusion that the absorption is red-shifted by increasing the π-conjugation chain length. On experiment, Suh et al. [11] observed the similar spectral shift trend, and they presumed that extra π-conjugation bond between two benzene rings in **PCPP** alters the overall optical properties in a way different from simple effective conjugation length consideration. But based on our calculations, the frontier molecular orbitals of **PCPP** and **PHCPP** have similar occupation characters. We found that the abnormal spectral shift trend can be interpreted by effective repeating unit (ERU) which is similar to the effective conjugation length (ECL). The ERU was estimated by the convergence of the excitation energies with the chain length within a threshold of 0.01 eV, based on the obtained binomial between the excitation energy and reciprocal chain length. The ERU of **PCPP** and **PHCPP** are estimated to be 9 and 14, respectively, so the π-conjugation effect of **PHCPP** is greater than that of **PCPP**. Thus, the absorption blue-shift of **PCPP** compared with **PHCPP** can also be interpreted by the well-known conclusion, but the π-conjugation chain length is strictly changed to effective π-conjugation length, namely, the absorption can be red-shifted by increasing ERU.

Interestingly, Fig. 6 shows that **CPP4** has two absorption peaks at 289 nm and 277 nm, but **HCPP4** has only one peak at 300 nm. Fig. 9b shows that the absorption band at 300 nm of **HCPP4** is assigned to $\pi \rightarrow \pi^*$ transition localized on the whole molecule frame but dominantly on the side repeating units with more than 60% composition. The absorption band at 277 nm of **CPP4** has similar $\pi \rightarrow \pi^*$ transition character to the absorption band at 300 nm of **HCPP4** (see Fig. 8c). And the blue-shift of the absorption band at 277 nm of **CPP4** compared with that at 300 nm of **HCPP4** can also be interpreted by ERU just like the lowest-lying absorption. Fig. 8b shows that the absorption at 289 nm of **CPP4** also can be attributed to $\pi \rightarrow \pi^*$ transition, but the extra π-conjugated C=C bonds between two benzene rings also contribute to the excitation, and the molecular orbitals concentrate on the middle two repeating units with more than 80% compositions. On experiment, Suh

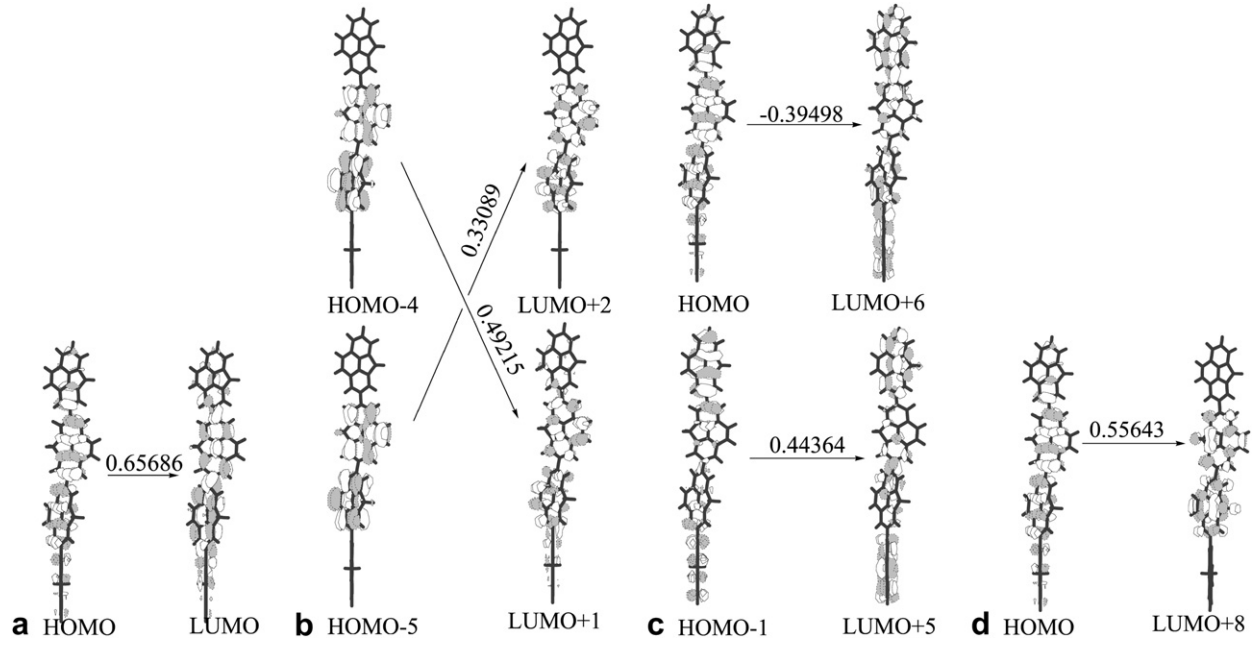

Fig. 8. The density diagram plots of the absorption at 344 nm (a), 289 nm (b), 277 nm (c), and 258 nm (d) of **CPP4** with |CI coefficient| > 0.1 under the TD-B3LYP calculations.

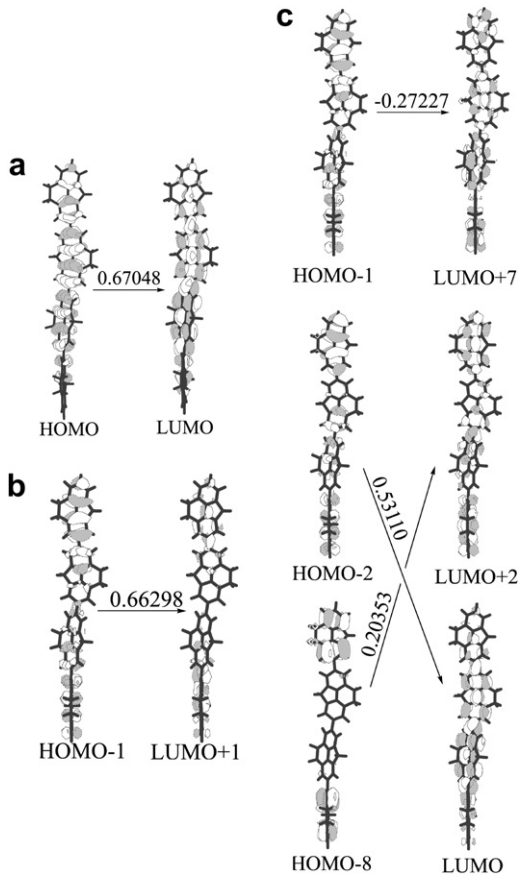

Fig. 9. The density diagram plots of the absorption at 371 nm (a), 300 nm (b), and 249 nm (c) of **HCPP4** with |CI coefficient| > 0.1 under the TD-B3LYP calculations.

et al. [11] also observed the extra absorption band of **PCPP** compared with **PHCPP**, and they presumed that the extra π-bonding between the two benzene rings in **PCPP** should be responsible for the extra absorption band by comparing chemical structures of **PCPP** and **PHCPP**. Based on theoretical calculation, we confirmed their presumption in the view of electronic structure. Other absorption bands given in Table 3 are all attributed to $\pi \rightarrow \pi^*$ transition without special characters (see Figs. 8 and 9).

3.5. The excited state geometries and the emissions

The main optimized excited state geometry parameters of **CPP***n* and **HCPP***n* are given in Table 1. The optimized geometries of **CPP4** and **HCPP4** are shown in Fig. 2. The optimized excited state geometries of **CPP***n* and **HCPP***n* ($n = 2$–4) have the similar screw structures to the ground state, but the screw degree becomes smaller, because the dihedral angle of C(7)–C(10)–C(14)–C(13) increases by about 20° compared with ground state. Other excited state dihedral angles C(3)–C(1)–C(2)–C(6)/C(1)–C(3)–C(4)–C(5)/C(3)–C(4)–C(5)–C(6) of **CPP***n* are hardly changed. But for **HCPP***n*, Table 1 shows that dihedral angles of C(3)–C(4)–C(5)–C(6) and C(1)–C(3)–C(4)–C(5) are greatly changed by about 30° and 40°, respectively, compared with the ground state, which indicates that the C–C single bond is distorted greatly. It is because the rigidity of C=C double bond is greater than that of C–C single bond, the C–C bond is easier to be distorted than the C=C bond by electronic excitation. The bond angles of **CPP***n* and **HCPP***n* are hardly changed by excitation. The C(1)–C(2)/C(4)–C(5)/C(9)–C(8)/C(9)–C(12)/C(10)–C(14) bonds become stronger, but C(3)–C(4)/C(5)–C(6) bonds become weaker compared with ground state results.

Table 4
The calculated fluorescence emissions of **PCPP** and **PHCPP** under the TD-B3LYP calculations, together with the experimental data

	Excited states	λ, nm (eV)	Config (CI coeff)	Oscillator	Relative weight (%)
CPP1	$^1\pi\pi^*$	308 (4.03)	H → L (0.62)	0.2096	78.5
CPP2	$^1\pi\pi^*$	358 (3.46)	H → L (0.64)	1.1888	83.6
CPP3	$^1\pi\pi^*$	380 (3.26)	H → L (0.66)	2.0083	88.9
CPP4	$^1\pi\pi^*$	393 (3.16)	H → L (0.66)	2.6591	88.9
HCPP1	$^1\pi\pi^*$	302 (4.11)	H → L (0.63)	0.3647	81.0
HCPP2	$^1\pi\pi^*$	387 (3.20)	H → L (0.64)	1.4467	83.6
HCPP3	$^1\pi\pi^*$	418 (2.97)	H → L (0.66)	2.2432	88.9
HCPP4	$^1\pi\pi^*$	432 (2.87)	H → L (0.66)	2.8666	88.9

The calculated fluorescence of **CPP***n* and **HCPP***n* as well as relative weight, configuration, and oscillator strength are summarized in Table 4. The calculated fluorescence are red-shifted in the order of **CPP1** (308 nm) < **CPP2** (358 nm) < **CPP3** (380 nm) < **CPP4** (393 nm) with the increase of the repeating units from 1 to 4, and **HCPP***n* have the similar red-shift trend to **CPP***n*. These fluorescence can be described as originating from $^1\pi\pi^*$ excited state more than 78.5% weight compositions. Through analyzing the transition configuration of the fluorescence, we found that the calculated fluorescence is just the reverse process of the lowest-lying absorption, since the emission and the lowest-lying absorptions have the same symmetries (A^1B) and transition characters ($X^1A \leftrightarrow A^1B$). The Stokes shifts between the calculated lowest-lying absorptions and emissions are 0.30, 0.35, 0.46, 0.44 eV for **CPP1**–**CPP4** and 0.60, 0.63, 0.51, 0.47 eV for **HCPP1**–**HCPP4**, respectively, and the modest shifts are in agreement with the slight change of the geometries from the ground state to the excited state. With the extrapolation method, we obtained the fluorescence of **PCPP** (432 nm, 2.87 eV) and **PHCPP** (470 nm, 2.64 eV). The fluorescence of **PCPP** is blue-shifted compared with that of **PHCPP** despite that **PCPP** has an extra π-conjugation C=C double bond between two benzene rings, which also can be interpreted by the fact that the ERU of **PCPP** (9) is smaller than that of **PHCPP** (14), and this fact can be seen from Fig. 3 that the frontier molecular orbitals of **HCPP4** (30.0%) localized on end repeating unit are more than that of **CPP4** (27.0%), thus, the π-conjugation effect of **PHCPP** is greater than that of **PCPP**. The calculated results showed that **PCPP** is a good blue-emitting material with remarkable color stability and rigid backbone.

4. Conclusions

The present work studied the geometries, electronic structures, IPs, EAs, absorption and fluorescence properties of two series oligomers **CPP***n* and **HCPP***n* ($n = 1$–4). **CPP***n* and **HCPP***n* show smooth binomial relationship between inverse repeating unit numbers ($1/n$) and the H–L gap, IPs, EAs, and the optical properties. By extrapolation method, we predicted the properties of **PCPP** and **PHCPP**. The lowest-lying absorption of **PCPP** and **PHCPP** are attributed to $\pi \rightarrow \pi^*$ transition, and the fluorescent emission can be described as originating from $^1\pi\pi^*$ excited state. The calculation results also revealed that the absorptions and the emissions are red-shifted with the increasing ERU but not with the increasing repeating unit number solely. The extra absorption band at 289 nm of **PCPP** is assigned to $\pi \rightarrow \pi^*$ transition involving the extra C=C bond between benzene rings. The calculated results showed that **PCPP** is suitable for blue-emitting LEDs.

Acknowledgment

This work is supported by the Natural Science Foundation of China (20173021, 20333050 and 20573042).

References

[1] (a) Brédas JL, Beljonne D, Coropceanu V, Cornil J. Chem Rev 2004;104:4971;
(b) Zhang X, Cote AP, Matzger AJ. J Am Chem Soc 2005;127:10502;
(c) Cho NS, Park JH, Lee SK, Lee J, Shim HK, Park MJ, et al. Macromolecules 2006;39:177;
(d) Castro FA, Graeff CFO, Heier J, Hany R. Polymer 2007;48:2380.

[2] (a) Brabec CJ, Sariciftci NS, Hummelen JC. Adv Funct Mater 2001;11:15;
(b) Jenekhe SAYS. Appl Phys Lett 2000;77:2635;
(c) Kim H, Kim JY, Park SH, Lee K, Jin Y, Kim J, et al. Appl Phys Lett 2005;86:183502.

[3] (a) Luo J, Li XZ, Hou Q, Peng JB, Yang W, Cao Y. Adv Mater 2007;19:1113;
(b) Leung LM, Liu CM, Wong CK, Kwong CF. Polymer 2002;43:233;
(c) Huang C, Zhen CG, Su SP, Vijila C, Balakrisnan B, Auch MDJ, et al. Polymer 2006;47:1820;
(d) Wang E, Li C, Mo YQ, Zhang Y, Ma G, Shi W, et al. J Mater Chem 2006;16:4133;
(e) Zeng WJ, Wu HB, Zhang C, Huang F, Peng JB, Yang W, et al. Adv Mater 2007;19:810;
(f) Rathnayake HP, Cirpan A, Delen Z, Lahti PM, Karasz FE. Adv Funct Mater 2007;17:115.

[4] (a) Ong BS, Wu Y, Liu P, Gardner S. J Am Chem Soc 2004;126:3378;
(b) Babel A, Jenekhe SA. J Phys Chem B 2003;107:1749;
(c) Babel A, Jenekhe SA. Adv Mater 2002;14:371;
(d) Katz HE. J Mater Chem 1997;7:369.

[5] (a) McQuade DT, Pullen AE, Swager TM. Chem Rev 2000;100:2537;
(b) Thomas III SW, Joly GD, Swager TM. Chem Rev 2007;107:1339;
(c) Grabchev I, Bosch P, McKenna M, Nedelcheva A. Polymer 2007;48:6755.

[6] Burroughes JH, Bradley DDC, Brown AR, Marks RN, Mackay K, Friend RH, et al. Nature 1990;347:539.

[7] (a) Grem G, Leditzky G, Ullrech B, Leising G. Adv Mater 1992;4:36;
(b) Cimrova V, Schmidt W, Rulkens R, Schulze M, Meyer W, Neher D. Adv Mater 1996;8:585;
(c) Yamamoto T, Arai M, Kokubo H, Sasaki S. Macromolecules 2003;36:7986;
(d) Yu WL, Pei J, Cao Y, Huang W, Heeger AJ. Chem Commun 1999:1837;
(e) Jin Y, Jee J, Kim K, Kim J, Song S, Park SH, et al. Polymer 2007;48:1541;
(f) Hendry E, Schins JM, Candeias LP, Siebbeles LDA, Bonn M. Phys Rev Lett 2004;92:196601;
(g) Prins P, Candeias LP, van Breemen AJJM, Sweelssen J, Herwig PT, Schoo HFM, et al. Adv Mater 2005;17:718;
(h) Claudio GC, Bittner ER. J Phys Chem A 2003;107:7092.

[8] (a) Pei Q, Yang Y. J Am Chem Soc 1996;118:7416;
(b) Yang CY, Heeger AJ, Cao Y. Polymer 2000;41:4113;
(c) Sun ML, Niu QL, Yang RQ, Du B, Liu RS, Yang W, et al. Eur Polym J 2007;43:1916;
(d) Lee J, Cho HJ, Jung BJ, Cho NS, Shim HK. Macromolecules 2004;37:8523;
(e) Jin JY, Jin ZZ, Xia Y, Zhou ZY, Wu X, Zhu DX, et al. Polymer 2007;48:4028;
(f) Du B, Liu RS, Zhang Y, Yang W, Sun WB, Sun ML, et al. Polymer 2007;48:1245.

[9] (a) Mo YQ, Jiang X, Cao DR. Org Lett 2007;9:4371;
(b) Lee JI, Klaerner G, Miller RD. Chem Mater 1999;11:1083;
(c) Marsitzky D, Murray J, Campbell Scott J, Carter KR. Chem Mater 2001;13:4285;
(d) Tapia MJ, Burrows HD, Valente AJM, Pradhan S, Scherf U, Lobo VMM, et al. J Phys Chem B 2005;109:19108;
(e) Tapia MJ, Burrows HD, Knaapila M, Monkman AP, Arroyo A, Pradhan S, et al. Langmuir 2006;22:10170.

[10] (a) List EJW, Guentner R, Freitas PS, Scherf U. Adv Mater 2002;14:374;
(b) Zojer E, Pogantsch A, Beljonne D, Brédas JL, List EJW. Chem Phys 2002;117:6794;
(c) Romaner L, Piok T, Gadermaier C, Guentner R, De Freitas PS, Scherf U, et al. Synth Met 2003;139:851.

[11] (a) Park SH, Jin Y, Kim JY, Kim SH, Kim J, Suh H, et al. Adv Funct Mater 2007;17:3063;
(b) Suh H, Jin Y, Park SH, Kim D, Kim J, Kim C, et al. Macromolecules 2005;38:6285.

[12] (a) Wang ZY, Su KH, Fan HQ, Wen ZY. Polymer 2007;48:7145;
(b) Delaere D, Nguyen MT, Vanquickenborne LG. J Phys Chem A 2003;107:838;
(c) Tang WH, Ke L, Tan LW, Lin TT, Kietzke T, Chen ZK. Macromolecules 2007;40:6164;
(d) Lei SB, Deng K, Yang YL, Zeng QD, Wang C, Ma Z, et al. Macromolecules 2007;40:4552;
(e) Grozema FC, van Duijnen PTh, Berlin YA, Ratner MA, Siebbeles LDA. J Phys Chem B 2002;106:7791;
(f) Poulsen L, Jazdzyk M, Communal JE, Sancho-García JC, Mura A, Bongiovanni G, et al. J Am Chem Soc 2007;129:8585.

[13] Lahti PM, Obrzut J, Karasz FE. Macromolecules 1987;20:2023.

[14] Miyata Y, Nishinaga T, Komatsu K. J Org Chem 2005;70:1147.

[15] (a) Ma J, Li SY, Jiang YS. Macromolecules 2002;35:1109;
(b) Wang YJ, Ma J, Jiang YS. J Phys Chem A 2005;109:7197;
(c) Zhang GL, Ma J, Jiang YS. J Phys Chem B 2005;109:13499.

[16] (a) Wang JF, Feng JK, Ren AM, Liu XD, Ma YG, Lu P, et al. Macromolecules 2004;37:3451;
(b) Liao Y, Feng JK, Yang L, Ren AM, Zhang HX. Organometallics 2005;24:385;
(c) Yang L, Ren AM, Feng JK, Wang JF. J Org Chem 2005;70:3009.

[17] Gierschner J, Cornil J, Egelhaaf HJ. Adv Mater 2007;19:173.

[18] Bryce AB, Charnochk JM, Pattrichk RAD, Lennie AR. J Phys Chem A 2003;107:2516.

[19] Pan QJ, Zhang HX. Eur J Inorg Chem 2003:4202.

[20] Naito K, Sakurai M, Egusa S. J Phys Chem A 1997;101:2350.

[21] (a) Liu LT, Yaron D, Sluch MI, Berg MA. J Phys Chem B 2006;110:18844;
(b) Lind P, Eriksson A, Lopes C, Eliasson B. J Phys Org Chem 2005;18:426.

[22] (a) Runge E, Gross EKU. Phys Rev Lett 1984;52:997;
(b) Parr RG, Yang W. Density functional theory of atoms and molecules. New York: Oxford University Press; 1989.

[23] (a) Casado J, Pappenfus TM, Mann KR, Ortì E, Viruela PM, Milian B, et al. Chem Phys Chem 2004;5:529;
(b) Milian B, Pou-Amerigo R, Viruela R, Orti E. Chem Phys Lett 2004;391:148.

[24] Becke AD. J Chem Phys 1993;98:5648.

[25] (a) Stephens PJ, Devlin FJ, Chabalowski FCF, Frisch MJ. J Phys Chem 1994;98:11623;
(b) Novoa JJ, Sosa C. J Phys Chem 1995;99:15837.

[26] Kertesz M, Choi CH, Yang SJ. Chem Rev 2005;105:3448.

[27] Raghavachari K, Pople JA. Int J Quantum Chem 1981;20:1067.

[28] Halls MD, Schlegel HB. Chem Mater 2001;13:2632.

[29] (a) Liu T, Gao JS, Xia BH, Zhou X, Zhang HX. Polymer 2007;48:502;
(b) Zhou X, Zhang HX, Pan QJ, Xia BH, Tang AC. J Phys Chem A 2005;109:8809;
(c) Pan QJ, Zhang HX. Organometallics 2004;23:5198.

[30] Foresman JB, Head-Gordon M, Pople JA, Frisch MJ. J Phys Chem 1992;96:135.

[31] Casida ME, Jamorski C, Casida KC, Salahub DR. J Chem Phys 1998;108:4439.

[32] (a) Stratmann RE, Scuseria GE. J Chem Phys 1998;109:8218;
(b) Matsuzawa NN, Ishitani A. J Phys Chem A 2001;105:4953.

[33] Frisch MJ, Trucks GW, Schlegel HB, Scuseria GE, Robb MA, Cheeseman JR, et al. Gaussian 03, revision C02. Wallingford CT: Gaussian Inc; 2004.

[34] Cohen R, Stokbro K, Martin JML, Ratner MA. J Phys Chem C 2007;111:14893.

[35] Fabiano E, Sala FD, Cingolani R, Weimer M, Görling A. J Phys Chem A 2005;109:3078.